JOC Article

Time Dependent Density Functional Theory Calculations for Electronic Circular Dichroism Spectra and Optical Rotations of Conformationally Flexible Chiral Donor−Acceptor Dyad

Tadashi Mori,*,†,‡ Yoshihisa Inoue,† and Stefan Grimme*,‡

Department of Molecular Chemistry, Graduate School of Engineering, Osaka University, 2-1 Yamada-oka, Suita 565-0871, Japan, and Theoretische Organische Chemie, Organisch-Chemisches Institut der Universität Münster, Corrensstrasse 40, D-48149 Münster, Germany

tmori@chem.eng.osaka-u.ac.jp

Received September 7, 2006

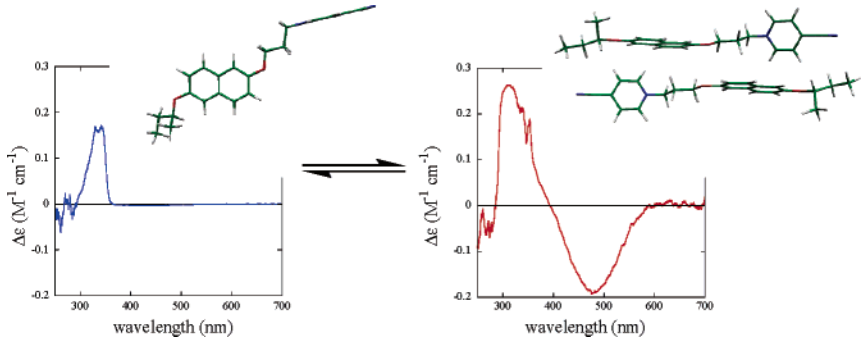

Twelve conformations of a chiral donor−acceptor (charge-transfer) dyad and six conformations of its dimer complex were structurally optimized by using the Kohn−Sham density functional theory (BLYP/TZV2P) incorporating a recently developed empirical correction scheme that uses C_6/R^6 potentials for van der Waals interactions (DFT-D). Subsequent time-dependent DFT calculations with BH-LYP and B3-LYP functionals (with triple-ζ basis set) were performed to obtain theoretical circular dichroism (CD) spectra. The experimental CD spectra obtained independently were properly reproduced by averaging the calculated spectra of individual conformers according to a Boltzmann population derived from single-point SCS-MP2 energies. The optical rotations of the monomer were also calculated by using the same functionals with an aug-cc-pVDZ basis set. Dielectric continuum solvation models (COSMO) applied to correct the relative energies from the isolated molecule calculations resulted in conformer distributions that piled the same or even poorer level of agreement with the experimental CD spectrum. Our results clearly show the advantage of the DFT-D method for the geometry optimization of large systems with donor−acceptor interactions and the TD-DFT/BH-LYP calculations for reproducing the experimental CD spectra. As compared with the calculated optical rotations, the wealthy information embedded in the experimental/calculated CD spectra is requisite for the configurational and/or conformational analyses of relatively large and flexible chiral organic molecules in solution.

1. Introduction

Electronic circular dichroism (CD)[1] is one of the fundamental properties of chiral molecules. CD spectroscopy measures the difference in molar extinction coefficient (ϵ) for left- and right-handed circularly polarized light ($\Delta\epsilon = \epsilon_l - \epsilon_r$). Reflecting the chiral nature of molecules, the method provides us with rich information about the conformational and configurational, as well as electronic, structures of the relevant molecule and its fragments. Several empirical relationships between chiral structure and chiroptical properties have been proposed and CD spectroscopy is a routine tool for elucidating the secondary/tertiary structure of proteins and nucleic acids.[2] For relatively simple organic molecules, a number of reliable rules have been

* Author to whom correspondence should be addressed. Fax: +81-6-6879-7923.
† Osaka University.
‡ Universität Münster.

(1) (a) Berova, N.; Nakanishi, K.; Woody, R. W. *Circular Dichroism, Principles and Applications*, 2nd ed.; John Wiley & Sons: New York, 2000. (b) Lightner, D. A.; Gurst, J. E. *Organic Conformational Analysis and Stereochemistry from Circular Dichroism Spectroscopy*; John Wiley & Sons: New York, 2000.

10.1021/jo061855i CCC: $33.50
Published on Web 11/29/2006

established to correlate the sign and magnitude of observed Cotton effects and the absolute configuration of chiral compound.[3] We have also employed CD spectroscopy in the analyses of configuration and conformation of (reactive) chemical species such as radical cations in solution.[4] Nevertheless, the relationship between molecular structure and the CD signals does not appear to be fully understood and the empirical rules are not very reliable particularly in less conventional cases. Indeed, we have recently revealed that one of the empirical methods fails to correctly predict the absolute configuration of simple donor−acceptor (CT) cyclophanes that exhibit bizarre CD spectra.[5] It is thus obvious that more accurate theoretical treatment of circular dichroism is indispensable for elucidating the observed chiroptical properties and also for establishing a more reliable general method for determining the absolute configurations of a wider range of chiral species.

Extension of density functional theory (DFT) to the time-dependent realm allows us to calculate the time- and frequency-dependent responses, such as excitation energies, polarizabilities, hyperpolarizabilities, and Raman activities, with comparable computational expenses and much higher accuracy than some of the more frequently used ab initio methods (RPA or CIS). Although the TD-DFT method was developed only about two decades ago, it has become one of the most prominent methods for calculating the excited-state properties of medium-to-large sized real molecules.[6] Consequently, the TD-DFT calculations of chiroptical properties such as optical rotations[7−9] and CD spectra[8,10] have recently been applied successfully to the absolute configuration assignment of small-to-medium organic molecules.

CHART 1. Chiral CT-Dyad

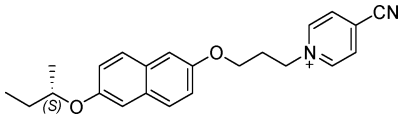

Although the calculation of optical rotatory dispersion (ORD) is more general (not requiring any chromophoric group in the common spectral region), the importance of the combined use of the circular dichroism and optical rotation (or dispersions) has recently been emphasized[11] for an accurate determination of the absolute configuration, especially when the specific rotation ($[\alpha]_D$) is not very large.[12]

One can find ample recent examples of calculated optical dispersions[11,13] and vibrational absorption spectra[14] applied to the conformational analysis of chiral molecules. In contrast, calculated CD spectra have not been employed in the conformational analysis of large molecules (with or without donor−acceptor interactions). In this first study we want to examine the reliability of calculated CD spectra for donor−acceptor complexes by the TD-DFT method. We have chosen a donor−acceptor (CT)-dyad, *N*-(((*S*)-1-methylpropyloxy)-2-naphthoxypropyl)-4-cyanopyridinium (Chart 1)[15] as a representative example, since this compound is known to exhibit remarkable conformational variations, depending on the conditions employed (such as temperature, concentration, and the presence of various host molecules). The CT interaction between a donor and an acceptor part is an important class of noncovalent interactions that has been extensively exploited for assembling the molecules and developing molecular architectures.[16] For the

(2) (a) Chen, E.; Goldbeck, R. A.; Kliger, D. S. *J. Phys. Chem. A* **2003**, *107*, 8149−8155. (b) Rogers, D. M.; Hirst, J. D. *Biochemistry* **2004**, *43*, 11092−11102. (c) Ozdemir, A.; Lednev, I. K.; Asher, S. A. *Biochemistry* **2002**, *41*, 1893−1896. (d) Mukerji, I.; Williams, A. P. *Biochemistry* **2002**, *41*, 69−77.

(3) For example, see: (a) Smith, H. E. *Chem. Rev.* **1998**, *98*, 1709−1740. (b) Moffitt, W.; Woodward, R. B.; Moscowitz, A.; Klyne, W.; Djerassi, C. *J. Am. Chem. Soc.* **1961**, *83*, 4013−4018. (c) Harada, N.; Nakanishi, K. *J. Am. Chem. Soc.* **1969**, *91*, 3989−3991. (d) Smith, H. E.; Neergaard, J. R.; Burrows, E. P.; Chen, F.-M. *J. Am. Chem. Soc.* **1974**, *96*, 2908−2916.

(4) (a) Mori, T.; Izumi, H.; Inoue, Y. *J. Phys. Chem. A* **2004**, *108*, 9540−9549. (b) Mori, T.; Inoue, Y. *J. Phys. Chem. A* **2005**, *109*, 2728−2740.

(5) Furo, T.; Mori, T.; Wada, T.; Inoue, Y. *J. Am. Chem. Soc.* **2005**, *127*, 8242−8243, 16338.

(6) (a) Grimme, S. *Rev. Comput. Chem.* **2004**, *20*, 153−218. (b) Dreuw, A.; Head-Gordon, M. *Chem. Rev.* **2005**, *105*, 4009−4037. (c) For an older review see: Polavarapu, P. L. *Chirality* **2002**, *14*, 768−781.

(7) (a) Grimme, S.; Furche, F.; Ahlrichs R. *Chem. Phys. Lett.* **2002**, *361*, 321−328. (b) Grimme, S. *Chem. Phys. Lett.* **2001**, *339*, 380−388.

(8) (a) McCann, D. M.; Stephens, P. J. *J. Org. Chem.* **2006**, *71*, 6074−6098. (b) Stephens, P. J.; McCann, D. M.; Devlin, F. J.; Smith, A. B., III *J. Nat. Prod.* **2006**, *69*, 1055−1064. (c) Stephens, P. J.; McCann, D. M.; Butkus, E.; Stoncius, S.; Cheeseman, J. R.; Frisch, M. J. *J. Org. Chem.* **2004**, *69*, 1948−1958.

(9) (a) Stephens, P. J.; McCann, D. M.; Cheeseman, J. R.; Frisch, M. J. *Chirality* **2005**, *17*, S52−S64. (b) Stephens, P. J.; Devlin, F. J.; Cheeseman, J. R.; Frisch, M. J.; Bortolini, O.; Besse, P. *Chirality* **2003**, *15*, S57−S64. (c) Stephens, P. J.; Devlin, F. J.; Cheeseman, J. R.; Frisch, M. J.; Rosini, C. *Org. Lett.* **2002**, *4*, 4595−4598. (d) Ruud, K.; Helgaker, T. *Chem. Phys. Lett.* **2002**, *352*, 533−539. (e) Autschbach, J.; Patchkovskii, S.; Ziegler, T.; van Gisbergen, S. J. A.; Baerends, E. J. *J. Chem. Phys.* **2002**, *117*, 581−592. (f) Stephens, P. J.; Devlin, F. J.; Cheeseman, J. R.; Frisch, M. J. *J. Phys. Chem. A* **2001**, *105*, 5356−5379.

(10) (a) Diedrich, C.; Grimme, S. *J. Phys. Chem. A* **2003**, *107*, 2524−2539. (b) Autschbach, J.; Ziegler, T.; van Gisbergen, S. J. A.; Baerends, E. J. *J. Chem. Phys.* **2002**, *116*, 6930−6940. (c) Furche, F.; Ahlrichs, R.; Wachsmann, C.; Weber, E.; Sobanski, A.; Vogtle, F.; Grimme, S. *J. Am. Chem. Soc.* **2000**, *122*, 1717−1724. (d) Autschbach, J.; Ziegler, T.; van Gisbergen, S. J. A.; Baerends, E. J. *J. Chem. Phys.* **2002**, *116*, 6930−6940. (e) Pecul, M.; Ruud, K.; Helgaker, T. *Chem. Phys. Lett.* **2004**, *388*, 110−119.

(11) (a) Tam, M. C.; Crawford, T. D. *J. Phys. Chem. A* **2006**, *110*, 2290−2298. (b) Stephens, P. J.; McCann, D. M.; Devlin, F. J.; Cheeseman, J. R.; Frisch, M. J. *J. Am. Chem. Soc.* **2004**, *126*, 7514−7521.

(12) (a) McCann, D. M.; Stephens, P. J.; Cheeseman, J. R. *J. Org. Chem.* **2004**, *69*, 8709−8717. (b) Autschbach, J.; Jensen, L.; Schatz, G. C.; Tse, Y. C. E.; Krykunov, M. *J. Phys. Chem. A* **2006**, *110*, 2461−2473.

(13) Kundrat, M. D.; Autschbach, J. *J. Phys. Chem. A* **2006**, *110*, 4115−4123.

(14) (a) Shin, S.; Nakata, M.; Hamada, Y. *J. Phys. Chem. A* **2006**, *110*, 2122−2129. (b) Vargas, A.; Bonalumi, N.; Ferri, D.; Baiker, A. *J. Phys. Chem. A* **2006**, *110*, 1118−1127. For a use of VCD spectra in absolute configuration determination, see for examples: (c) Fristrup, P.; Lassen, P. R.; Johannessen, C.; Tanner, D.; Norrby, P.-O.; Jalkanen, K. J.; Hemmingsen, L. *J. Phys. Chem. A* **2006**, *110*, 9123−9129. (d) Carosati, E.; Cruciani, G.; Chiarini, A.; Budriesi, R.; Ioan, P.; Spisani, R.; Spinelli, D.; Cosimelli, B.; Fusi, F.; Frosini, M.; Matucci, R.; Gasparrini, F.; Ciogli, A.; Stephens, P. J.; Devlin, F. J. *J. Med. Chem.* **2006**, *49*, 5206−5216. (e) Tarczay, G.; Magyarfalvi, G.; Vass, E. *Angew. Chem., Int. Ed.* **2006**, *45*, 1775−1777. (f) Brotin, T.; Cavagnat, D.; Dutasta, J.-P.; Buffeteau, T. *J. Am. Chem. Soc.* **2006**, *128*, 5533−5540. (g) Monde, K.; Taniguchi, T.; Miura, N.; Vairappan, C. S.; Suzuki, M. *Chirality* **2006**, *18*, 335−339. (h) Naubron, J.-V.; Giordano, L.; Fotiadu, F.; Buergi, T.; Vanthuyne, N.; Roussel, C.; Buono, G. *J. Org. Chem.* **2006**, *71*, 5586−5593. (i) Devlin, F. J.; Stephens, P. J.; Besse, P. *J. Org. Chem.* **2005**, *70*, 2980−2993. (j) Devlin, F. J.; Stephens, P. J.; Besse, P. *Tetrahedron*: *Asymmetry* **2005**, *16*, 1557−1566. Devlin, F. J.; Stephens, P. J.; Bortolini, O. *Tetrahedron*: *Asymmetry* **2005**, *16*, 2653−2663. (k) Devlin, F. J.; Stephens, P. J.; Scafato, P.; Superchi, S.; Rosini, C. *Chirality* **2002**, *14*, 400−406. (l) Devlin, F. J.; Stephens, P. J.; Oesterle, C.; Wiberg, K. B.; Cheeseman, J. R.; Frisch, M. J. *J. Org. Chem.* **2002**, *67*, 8090−8096. (m) Stephens, P. J.; Devlin, F. J.; Aamouche, A. *ACS Symp. Ser.* **2002**, *810*, 18−33. (n) Aamouche, A.; Devlin, F. J.; Stephens, P. J. *J. Am. Chem. Soc.* **2000**, *122*, 2346−2354.

(15) (a) Mori, T.; Ko, Y. H.; Kim, K.; Inoue, Y. *J. Org. Chem.* **2006**, *71*, 3232−3247. (b) Mori, T.; Inoue, Y. *Angew. Chem., Int. Ed.* **2005**, *44*, 2582−2585.

(16) (a) Rosokha, S. V.; Kochi, J. K. *J. Org. Chem.* **2002**, *67*, 1727−1737. (b) Hubig, S. M.; Lindeman, S. V.; Kochi, J. K. *Coord. Chem. Rev.* **2000**, *200*−*202*, 831−873. (c) Ko, Y.-H.; Kim, K.; Kang, J.-K.; Chun, H.; Lee, J. W.; Sakamoto, S.; Yamaguchi, K.; Fettinger, J. C.; Kim, K. *J. Am. Chem. Soc.* **2004**, *126*, 1932−1933. (d) Jeon, Y. J.; Bharadwaj, P. K.; Choi, S. W.; Lee, J.W.; Kim, K. *Angew. Chem., Int. Ed.* **2002**, *41*, 4474−4476.

present CT-dyad, we can manipulate the monomer−dimer complex equilibrium simply by changing the temperature, and can investigate the chiroptical properties of both species. The target molecule employed herein contains an enantiopure alkyl group with *S* configuration at a distant position.

It is well-documented that common Kohn−Sham density functionals which treat electron correlation only in an approximate manner cannot describe the van der Waals (vdW) or the CT interactions properly,[17] while the Møller−Plesset perturbation theory (MP2), which represents the most widely applied ab initio approach for weakly bound complexes, tends to overestimate the interaction energies and to underestimate intermolecular distances.[18] More sophisticated methods based on coupled-cluster theory such as CCSD(T) or QCISD(T)[19] are computationally not feasible for large or even medium-sized systems. We have recently developed the empirical correction scheme in efficient DFT calculation by adding pairwise C_6/R^6 potentials for vdW interactions (DFT-D method). This dispersion-corrected DFT method is a very efficient practical alternative to the electron-correlated methods and has been successfully applied to a weakly bound intermolecular complexes[20] as well as a relatively large host−guest (tweezers) molecule.[21] Therefore, the geometries and binding energies of the present donor−acceptor system (the CT-dyad containing 27 non-hydrogen atoms) were investigated by using the DFT-D method in combination with the BLYP functional and basis sets of TZV2P quality. The TD-DFT method with hybrid-functionals incorporating different amounts of exact exchange (BH-LYP[22] and B3-LYP) was employed in the calculation of circular dichroism and optical rotation of each optimized conformer.[23] For consistency, the same functionals and equilibrium geometries are used for the specific rotation calculations.

We will show that the chosen method (BH-LYP/TZV2P) can nicely reproduce the experimental CD spectra of several different conformers of the monomer as well as dimer. This is in contrast to the more widely used optical rotation (OR) calculations, which involve similar computational efforts but lead to insufficient information on the conformation. The TD-DFT calculated CD spectra can be used as a "*fingerprint*" of each conformational variant of a large chiral molecule.

2. Computational Details

All calculations were performed on a LINUX-PC with the TURBOMOLE 5.6 program suite.[24] The resolution of identity (RI) approximation[25,26] was employed in all DFT-D-BLYP calculations, and the corresponding auxiliary basis sets were taken from the TURBOMOLE basis set library. The program modules escf,[27] cc2,[26] and mrci[28] have been used in the TD-DFT, coupled-cluster (CC2), and DFT/MRCI treatments. For CC2 assignments of the transitions are based on energy and transition moments since the current implementation does not allow the determination of configuration contributions. All 12 conformers were fully optimized at the dispersion-corrected DFT-D-BLYP level[29] without symmetry constraints, using an AO basis set of valence triple-ζ quality with two sets of polarization functions (2d2p, denoted as TZV2P; in standard notation: H, [3s2p], C/O, [5s3p2d]) and numerical quadrature multiple grid (m4 in Turbomole terminology). Subsequent single-point energy calculations were performed with the spin-component-scaled (SCS)-MP2 method[30,31] with a TZVPP basis set that has additional f and d functions on non-hydrogen and hydrogen atoms, respectively. It has been shown that a simple modification of the standard MP2 scheme, termed SCS-MP2, leads to dramatic improvements in accuracy, particularly on the molecules with weak interactions. The method is expected to provide the most accurate relative energies and was thus used to obtain the final Boltzmann distribution of the conformers. All excited-state calculations have been performed at the optimized ground-state geometries. The results thus correspond to vertical transitions, and the excitation energies can be approximately identified as the band maxima in the experimental spectra. The CD (and UV−vis) spectra were simulated on the basis of time-dependent density functional theory (TD-DFT) with both B3-LYP and BH-LYP functionals and employing the TZV2P basis set. We were unable to check the basis set incompleteness effects because of the size of the molecule, but the differences between length and velocity-gauge representations, which indicates sufficient basis set saturation, are found to be very small (within 0.1×10^{-40} cgs unit). The CD spectra were simulated by overlapping Gaussian functions for each transition where the width of the band at 1/*e* height is fixed at 0.4 eV and the resulting intensities of the combined spectra were scaled to the experimental values. As usual, the calculated band intensities are larger than their experimental counterparts. The somewhat smaller scaling factor used (1/10−1/20 instead of normally 1/2−1/3) is probably due to a more complete cancellation of the CD bands between the various conformers under the experimental conditions. A very small scaling factor (1/100) was used for the folded conformer(s), since the relative distributions under the experimental conditions are much lower (<5%). Due to a systematic overestimation of the transition

(17) Rappé, A. K.; Bernstein, E. R. *J. Phys. Chem. A* **2000**, *104*, 6117−6128.

(18) (a) van Mourik, T.; Karamertzanis, P. G.; Price, S. L. *J. Phys. Chem. A* **2006**, *110*, 8−12. (b) Sinnokrot, M. O.; Valeev, W. F.; Sherrill, C. D. *J. Am. Chem. Soc.* **2002**, *124*, 10887−10893. (c) Hobza, P.; Selzle, H. L.; Schlag, E. W. *J. Phys. Chem.* **1996**, *100*, 18790−18794.

(19) Helgaker, T.; Jørgensen, P.; Olsen, J. *Molecular Electronic-Structure Theory*; John Wiley & Sons: New York 2000.

(20) (a) Piacenza, M.; Grimme, S. *J. Am. Chem. Soc.* **2005**, *127*, 14841−14848. (b) Piacenza, M.; Grimme, S. *Chem. Phys. Chem.* **2005**, *6*, 1554−1558.

(21) Parac, M.; Etinski, M.; Peric, M.; Grimme, S. *J. Chem. Theory Comput.* **2005**, *1*, 1110−1118.

(22) Notations from Gaussian package correspond to BH&HLYP. See also: (a) Maity, D. K.; Duncan, W. T.; Truong, T. N. *J. Phys. Chem. A* **1999**, *103*, 2152−2159. (b) Duncan, W. T.; Truong, T. N. *J. Chem. Phys.* **1995**, *103*, 9642−9652. (c) Liao, M.-S.; Lu, Y.; Scheiner, S. *J. Comput. Chem.* **2003**, *24*, 623−631.

(23) It has been pointed out that TD-DFT gives substantial systematic errors in excitation energies for CT states and popular B3-LYP and related functionals failed to properly describe the structure and electronic states of the CT complexes, while there are successful examples of geometrical optimization of the intermolecular CT complexes by using the Becke's half-and-half (BH-LYP) functional. (a) Dreuw, A.; Fleming, G. R.; Head-Gordon, M. *J. Phys. Chem. B* **2003**, *107*, 6500−6503. (b) Tozer, D. J.; Amos, R. D.; Handy, N. C.; Roos, B. J.; Serrano-Andres, L. *Mol. Phys.* **1999**, *97*, 859−868. (c) Sobolewski, A. L.; Domcke, W. *Chem. Phys.* **2003**, *294*, 73−83. (d) Dreuw, A.; Head-Gordon, M. *J. Am. Chem. Soc.* **2004**, *126*, 4007−4016. (e) Dreuw, A.; Weisman, J. L.; Head-Gordon, M. *J. Chem. Phys.* **2003**, *119*, 2943−2946.

(24) Ahlrichs, R.; et. al. *TURBOMOLE*, version 5.6; Universität Karlsruhe: Karlsruhe, 2003. See also: http://www.cosmologic.de/QuantumChemistry/main_turbomole.html.

(25) (a) Eichkorn, K.; Treutler, O.; Öhm, H.; Häser, M.; Ahlrichs, R. *Chem. Phys. Lett.* **1995**, *240*, 283−289. (b) Weigend, F.; Häser, M. *Theor. Chem. Acc.* **1997**, *97*, 331−340. (c) Grimme, S.; Waletzke, M. *Phys. Chem. Chem. Phys.* **2000**, *2*, 2075−2081. (d) Vahtras, O.; Almlöf, J.; Feyereisen, M. W. *Chem. Phys. Lett.* **1993**, *213*, 514−518.

(26) Hättig, C.; Weigend, F. *J. Chem. Phys.* **2000**, *113*, 5154−5161.

(27) Bauernschmidt, R.; Ahlrichs, R. *Chem. Phys. Lett.* **1996**, *256*, 454−464.

(28) Grimme, S.; Waletzke, M. *J. Chem. Phys.* **1999**, *111*, 5645−5655.

(29) Grimme, S. *J. Comput. Chem.* **2004**, *25*, 1463−1473.

(30) (a) Grimme, S. *J. Phys. Chem. A* **2005**, *109*, 3067−3077. (b) Goumans, T. P. M.; Ehlers, A. W.; Lammertsma, K.; Würthwein, E.-U.; Grimme, S. *Chem. Eur. J.* **2004**, *10*, 6468−6475. (c) Grimme, S. *J. Chem. Phys.* **2003**, *118*, 9095−9102.

(31) (a) Grimme, S. *J. Comput. Chem.* **2003**, *24*, 1529−1537. (b) Piacenza, M.; Grimme, S. *J. Comput. Chem.* **2004**, *25*, 83−99. (c) Gerenkamp, M.; Grimme, S. *Chem. Phys. Lett.* **2004**, *392*, 229−235.

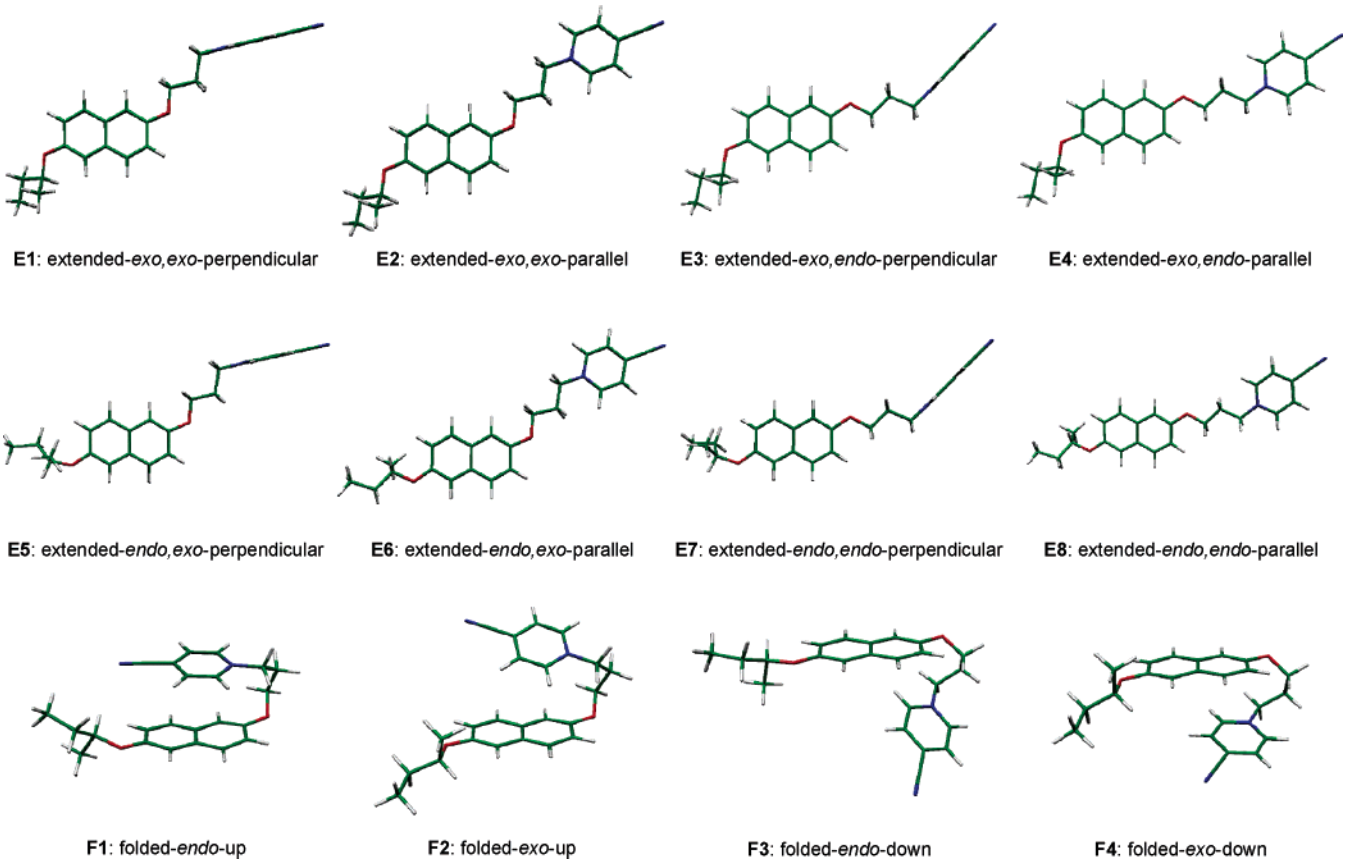

FIGURE 1. DFT-D-BLYP/TZV2P optimized structures of 12 conformations of the CT-dyad monomer.

energies in the BH-LYP calculations, the spectra were uniformly shifted by 0.5 eV unless otherwise stated (refers to B3-LYP functionals). See ref 10 for more theoretical details on the simulation of CD spectra. The optical rotations were calculated at BH-LYP/aug-cc-pVDZ and B3-LYP/aug-cc-pVDZ levels for the same optimized structures. Rotational strengths are calculated by using both length and velocity representations; but the values from length-gauge representation were used throughout the text. It is known that in the absence of GIAOs, these are origin-dependent and origin-independent, respectively. Strictly speaking, the calculated optical rotations can only be compared to experimental values when they are origin-independent, but the length and velocity rotational strengths converge to the same value in the complete basis set limit. With our relatively large triple-ζ type AO basis sets, the differences between both representations are negligible. Several other quantum chemical methods (HF, DFT with two hybrid functionals, DFT/MRCI and CC2) have been tested for the CD spectrum of most stable extended conformer (**E1**) with a smaller basis set of SV(P) (a slightly larger SVP basis-set was employed for the CC2 calculation) in order to ensure the validity of our TD-DFT approach.

All dimer structures were constructed by dimerization in a head-to-tail fashion, using the three most stable extended monomers (**E1**−**E3**; population >5%). Six conformers were obtained as local minima when two monomer molecules were associated from both less hindered and hindered faces, respectively. The structures were fully optimized at the DFT-D/BLYP level as for the monomers with C_2 symmetry constraints. The subsequent SCS-MP2/TZVPP energies were used for the final Boltzmann distribution of the conformers, and among six conformers, three most stable conformers were subjected to further CD (and UV−vis) calculations at BH-LYP/TZV2P and B3-LYP/TZV2P levels.

The effect of the solvent on the distribution of the conformers was also addressed by application of the conductor-like screening model (COSMO).[32] All single-point energy calculations were performed with COSMO as implemented in the TURBOMOLE program suite. The dielectric constant (ϵ) of 36.64 and 8.93 (in acetonitrile and dichloromethane, respectively) and optimized atomic radii (C, 2.00 Å; N, 1.83 Å; O, 1.72 Å; H, 1.30 Å) for the construction of the molecular cavity were used for the calculations of both monomers and dimers. Note that the COSMO approach to solvent effects only considers basic electrostatic interactions but neglects, e.g., explicit solvation or specific interaction of the solute and furthermore ignores vdW/CT interactions.

3. Results and Discussion

Geometrical Optimization of CT-Dyad Monomer. Figure 1 displays all of the DFT-D/BLYP optimized monomer conformations of the CT-dyad (**E1**−**E8** and **F1**−**F4**).[33] The first eight conformers involve an extended conformation with respect to the donor and acceptor moieties. In these conformations, all of the methylene linkers are located in the *anti* orientation, while the donor and acceptor rings are either perpendicular or parallel to each other. The two alkyl groups in bisalkoxynaphthalene can be located in one of the two directions with respect to the long axis of the naphthalene moiety, represented as *exo* and

(32) (a) Klamt, A.; Schürmann, G. P. *J. Chem. Soc., Perkin Trans. 2* **1993**, 799−805. (b) Tomasi, J.; Persico, M. *Chem. Rev.* **1994**, *94*, 2027−2094. (c) Sinnecker, S.; Rajendran, A.; Klamt, A.; Diedenhofen, M.; Neese, F. *J. Phys. Chem. A* **2006**, *110*, 2235−2245.

(33) There exists a pair of rotational conformations around the *O*−*C*(chiral) and *C*(chiral)−*C*(ethyl) bond in the chiral alkyl groups (i.e., *trans*, *gauche* 1, and *gauche* 2). Thus 9 conformations could be possible for each conformer (**E1**−**E8** and **F1**−**F4**) presented in this study. However, the effect on the calculated UV−vis and CD spectra of such conformations turned out to be very small. Details will be described elsewhere.

TABLE 1. Conformational Energies and Populations of Extended and Folded Monomer of the CT-Dyad

conformer	ΔE (DFT-D)[a]	% population (DFT-D)[b]	ΔE_{vdW}[c]	$\Delta\Delta E_{vdW}$[d]	r(D−A)[e]	μ[f]	ΔE (SCS-MP2)[g]	% population (SCS-MP2)[b]	[α]/BH-LYP[h]	[α]/B3-LYP[h]
E1	1.01	54.2	26.7	0.04	9.9	5.96	2.48	61.7	+69.8	−131
E2	2.16	17.2	26.7	0.08	10.0	6.18	3.77	17.1	+49.7	+16.2
E3	2.24	15.9	26.7	0.02	10.0	6.88	4.08	12.5	+70.5	−140
E4	3.47	4.7	26.7	0.05	10.2	6.76	5.36	3.5	+41.8	+20.4
E5	5.37	0.7	27.4	0.77	9.9	6.64	7.58	0.4	+82.2	−1084
E6	3.29	5.6	26.7	0.02	10.0	6.80	5.19	4.1	+21.1	+31.7
E7	6.90	0.2	27.3	0.68	10.0	6.04	9.94	0.0	+37.3	−74.6
E8	4.61	1.5	26.6	≡0	10.2	6.17	6.95	0.7	+34.1	+95.3
F1	≡0	39.6	39.9	13.28	3.6	3.64	≡0	48.4	+312	−251
F2	0.18	33.0	34.6	7.93	4.5	4.35	0.60	26.5	−616	+2283
F3	2.07	5.0	32.7	6.07	5.1	4.93	3.27	1.8	−1084	−1659
F4	0.57	22.4	36.2	9.60	4.2	3.25	0.73	23.3	−2.9	−364

[a] Relative DFT-D-BLYP energy with TZV2P basis-set in kcal/mol. [b] Boltzmann distribution among the extended or folded monomers. [c] Dispersion energies calculated as the difference between energies of DFT-D-BLYP and DFT-BLYP (without dispersion correction). [d] Differential ΔE_{vdW} energies, i.e., contribution to the relative energies. [e] Distance between centers of donor and acceptor rings in angstroms. [f] Calculated dipole moment in debye. [g] Relative SCS-MP2/TZVPP energies for DFT-D optimized structures in kcal/mol. [h] Optical rotations calculated by TD-DFT with the aug-cc-pVDZ basis set.

TABLE 2. Comparison of Excited-State Properties Calculated by Several Methods for the Most Stable Extended Conformer E1 of the CT-Dyad

		HF	DFT/BH-LYP	DFT/B3-LYP	DFT/MRCI	CC2[b]
first	energy, eV	4.78	4.33	3.50	4.50	4.03
	osc. str.[a]	0.0748	0.0622	0.00001	0.0964	0.0535
	rot. str.[a]	3.2	3.0	≈0	3.8	3.9
	main transition(s)	96→98 (83.5%), 95→100 (12.6%)	96→98 (86.2%)	96→97 (99.8%)	96→98 (73.7%)	n.d.[c]
	classification	$\pi-\pi^*$	$\pi-\pi^*$	CT	$\pi-\pi^*$	$\pi-\pi^*$[d]
second	energy, eV	5.00	4.89	3.89	5.4	5.05
	osc. str.[a]	0.0035	0.0023	0.0512	0.0008	0.0039
	rot. str.[a]	0.07	0.3	2.8	−0.01	−0.02
	main transition(s)	95→98 (52.7%), 96→100 (41.0%)	95→98 (54.3%), 96→100 (39.6%)	96→98 (89.5%)	96→97 (87.0%)	n.d.[c]
	classification			$\pi-\pi^*$	CT	CT[d]
third	energy, eV	5.55	5.22	4.24	5.35	5.09
	osc. str.[a]	0.2629	0.00004	0.0003	0.0237	0.0748
	rot. str.[a]	−0.2	≈0	≈0	1.5	1.4
	main transition(s)	94→97 (71.8%), 93→99 (19.9%)	96→97 (99.8%)	96→99 (99.8%)	92→97 (56.5%), 94→99 (34.6%)	n.d.[c]
	classification		CT			

[a] Rotatory (atomic unit) and oscillator strengths (10^{-40} in cgs unit) reported in length-gauge representation. [b] With SVP basis set (instead of SV(P) basis set). [c] Not determined. [d] Assignment was based on the comparison of the oscillator strength with other methods.

endo. The relative DFT-D energies of the conformers are listed in Table 1, along with the mean donor−acceptor distances, calculated dipole moments, and single-point SCS-MP2 relative energies. All of the extended conformers possess relatively long donor−acceptor distances of ca. 10 Å with modest dipole moments of 6−7 debyes.

In addition to the extended ones, four folded conformers (**F1**−**F4**) were obtained upon optimization at the DFT-D-BLYP level. In these conformers, distance between donor and acceptor rings becomes much shorter (3.6−5.1 Å) than for the extended conformers and the most closely stacked **F1** is found the most stable conformation. In the other three folded conformations, the donor and acceptor moieties are not totally face-to-face stacked but are oriented in a near-perpendicular fashion. Interestingly, the calculated dipole moments for the folded conformers are significantly smaller (2−3 debye), although the acceptor moiety carries a (formal) positive charge on the nitrogen. Quite large interaction energies (ΔE = 6−13 kcal/mol) were found in all the folded conformers, while such stabilization was not observed at all for the extended conformations. The overall preference for the folded conformers over the extended ones in the gas phase is ascribed mostly to these large vdW stabilization energies for which the dispersion term is responsible.

The SCS-MP2 and DFT-D methods gave comparable relative energies and the same stability sequence for all of the extended and folded conformers. A reasonable agreement between these two methods justifies an applicability of the DFT-D method for the geometry optimization of the present system.[30] This demonstrates the excellent performance of the less-expensive DFT-D method and emphasizes the need for vdW corrections even for the interactions in charged systems.

Validation of Methods. Three single-reference approaches (TD-HF, TD-DFT, and CC2) and a multireference method (DFT/MRCI) were used to compare the CD/UV−vis spectra of the most stable extended conformer (**E1**) as a representative case. In the TD-DFT calculations, two different functionals (B3-LYP and BH-LYP) with different fraction of exact exchange in the functional (20% or 50%, respectively) were employed to examine in particular the degree of deviation in excitation energy of the charge-transfer transition (Table 2). In the TD-HF approach (100% exact exchange), a systematic overestimation of the excitation energy was found, as pointed out previously.[23] Note that the lowest CT excitation appears as the 14th transition

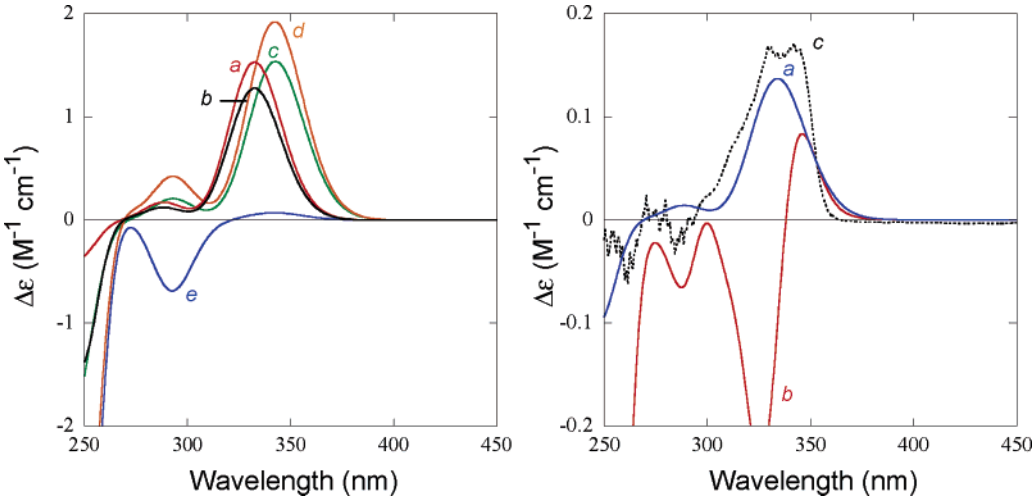

FIGURE 2. Left: Calculated CD spectra at the BH-LYP/TZV2P level for the most abundant extended conformers: (a) **E1**, (b) **E2**, (c) **E3**, (d) **E4**, and (e) **E6**. Note that the calculated spectra of less contributing **E5**, **E7**, and **E8** are omitted for clarity. Right: (a) A simulated CD spectrum obtained by a weighted average of all of the extended conformers with scaled intensity (1/10). (b) Averaged simulated CD spectrum with all the extended and folded conformers (scaled intensity 1/100). (c) Experimental CD spectrum in acetonitrile at 25 °C (path length = 0.2 cm).

(transition energy = 8.00 eV) in this calculation. The admixture of local exchange in the hybrid functionals (BH-LYP and B3-LYP) gradually lowers the excitation energy (of the lowest transition). Thus, the CT transition is found only as the third transition at the BH-LYP level, while this appears as the first transition at the B3-LYP level, revealing a larger underestimation of the CT excitation energy with the latter functional. By taking the DFT/MRCI or CC2 values as reference, all methods correctly predict the sign of the rotatory strength of the $\pi-\pi^*$ transition, although the magnitudes are predicted much smaller with the HF/DFT methods (at least with this basis set). Although the effect of the fraction of exact exchange for the monomer is not clear, the use of B3-LYP functional for the dimer apparently gave unacceptable results (vide infra).[34] Taking everything into consideration, we will primarily adopt the BH-LYP/TZV2P results for theoretical CD spectra in the following discussion. Results with the B3-LYP functional are used only for presenting the rotatory strength of the CT transition, for which the sign is usually predicted correctly (since the transition is always buried among other strong $\pi-\pi^*$ transitions with BH-LYP functional), but one should be cautious in dealing with the excitation energies that are always underestimated with this functional.

Calculation of CD Spectra with BH-LYP Functional. Theoretical CD spectra, which were calculated for the extended conformers with the BH-LYP/TZV2P functional, are shown in Figure 2 (left). It is interesting to note that conformers **E1**−**E4** give quite similar CD spectral patterns particularly for the first $\pi-\pi^*$ transition at ca. 340 nm (with slight variations in rotatory strength). Only the minor conformers, in which the chiral alkoxy group is in the *endo* orientation with respect to the longer axis of the naphthalene unit, display different CD profiles, as exemplified for **E6** in Figure 2 (data for **E5**, **E7**, and **E8** are not shown for clarity). However, these minor conformers do not appreciably affect the overall CD profiles due to their much smaller populations. An averaged CD spectrum of the extended conformers, which is weighted by their population calculated from the relative SCS-MP2 energies, is shown in Figure 2 (right), along with the experimental one. The effect of the counteranion in the experimental spectra was shown to be very small in the previous study.[15] The positive Cotton effect at around 340 nm is nicely reproduced by the theory, as a consequence of the mutually resembling CD profiles of the most contributing conformers **E1**−**E4**. The averaged spectrum was essentially the same as the one obtained when only major three conformers **E1**−**E3** are taken into consideration.

However, once the energetically more favored folded conformers are taken into account, the simulation differs completely from the experimental spectrum as shown in Figure 2 (right; red line) (see also Figure S1 (left) in the Supporting Information for the individual CD spectra of **F1**−**F4**), implying that such conformers are not populated under the experimental conditions (in solution). This clearly indicates that the calculated stabilities of the folded conformers in the gas phase are apparently overestimated relative to those of the extended conformers. This is because the cationic character of the acceptor moiety and the extended conformations should be more stabilized by the solvation. This tendency is slightly improved by considering the solvent effect on the conformer distribution (vide infra). However, among the extended conformers, such effects are much less and do not appreciably affect the overall shape of the spectrum.

Calculation of the Rotatory Strength of the CT Transition with the B3-LYP Functional. As mentioned previously, the simulated CD/UV−vis spectra with the B3-LYP functional are not always in good agreement with the experimental ones. Nevertheless, the simulated spectrum of the monomer reproduces the experimental one very well with a fairly small energy shift of 0.1 eV. In addition, the underestimation of the ΔE value, particularly for the CT excitation, turned out to be useful to distinguish this transition from the other high-energy transitions. We therefore address the theoretical Cotton effect of the CT band with this functional at this juncture. The calculated CD spectra of the folded conformers are shown in Figure 3 (left) and the averaged spectrum, weighted by the Boltzmann distribution based on the SCS-MP2 energies, is compared with the

(34) Details of the comparison of BH-LYP and B3-LYP functionals for the monomer and the dimer CT-dyad can be found in the Supporting Information. Calculations on several other systems with vdW/CT interactions with the BH-LYP functional always give better results than with the B3-LYP functional. Details will be published elsewhere.

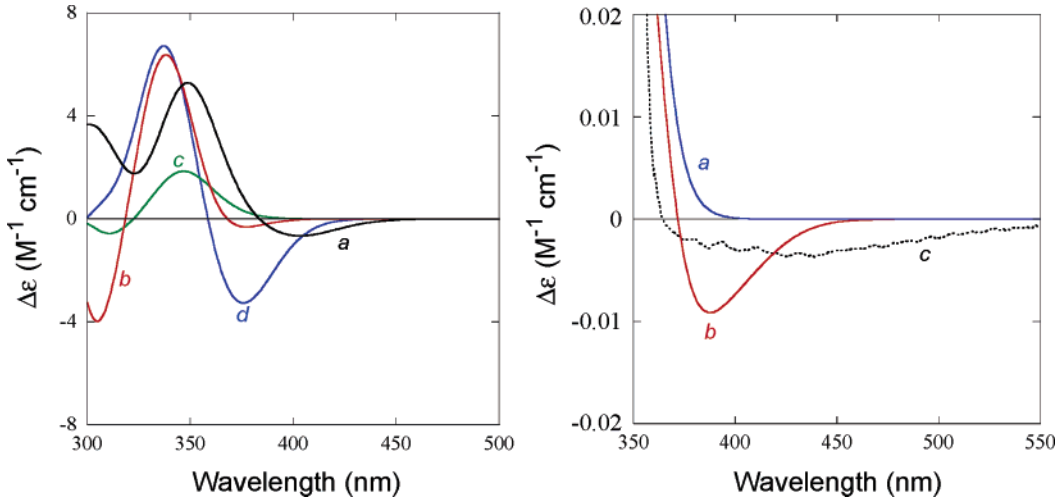

FIGURE 3. Left: CD spectra calculated at the B3-LYP/TZV2P level for the folded conformers with 0.1 eV red-shift: (a) **F1**, (b) **F2**, (c) **F3**, and (d) **F4**. Right: (a) CD spectrum simulated by averaging the extended conformers (scaled by 1/10). (b) CD spectrum simulated by averaging all the extended and folded conformers (scaled by 1/100). (c) Experimental CD spectrum in acetonitrile at 25 °C (path length = 10 cm).

experimental spectrum (Figure 3, right). Individual spectra of the extended conformers with this functional can be found in the Supporting Information (Figure S1, right). Note that the most stable conformer **F1** exhibits the negative Cotton effect at much longer wavelengths (~400 nm) than other conformers, which also principally contributes to the shape of the averaged spectrum (trace b in Figure 3, right).

The simulated spectrum with the B3-LYP functional also reproduces the experimental CD spectrum very well only if the extended conformers are considered. Note that the weak negative Cotton effect observed experimentally at ~420 nm is reproduced by the theory only when one considers the contribution of the folded conformers. This also supports the previous conclusion that small proportions of the folded conformers are present in solution as judged from the ROESY experiment.[15] In addition, the absolute value of the calculated rotatory strength in the CT band region is much larger than the experimental one, which clearly indicates that the population of the folded monomer in solution is very small (<5%).

Calculation of Optical Rotations. A number of recent papers describe the use of the TD-DFT method for the determination of absolute configuration of chiral molecules by calculating the specific rotation or rotatory dispersion.[7] In this context, it seems interesting to check the performance of such calculations applied to a donor−acceptor system and discuss the significance of the obtained results in comparison to the calculated CD spectra.

We have performed computations with the BH-LYP and B3-LYP functionals using the Dunning's aug-cc-pVDZ basis sets.[35] This roughly corresponds to the same or slightly smaller number of atomic orbitals (846 versus 873 used in TZV2P), but the calculation of specific rotation is more demanding in terms of computational time mainly because of the diffuse functions in the aug-cc-pVDZ basis set. The calculated $[\alpha]_D$ values thus obtained are also gathered in Table 1. With the B3-LYP functional, the values are rather sluggish and scattered even among the similar conformers. The failure of this functional for the present system is probably due to the significant underestimation of the charge-transfer transitions which are close to the wavelength of the sodium D-line (589.3 nm), that defectively affected the calculated optical rotation. The calculated $[\alpha]_D$ values with BH-LYP functional are more reliable in the present case (as was the case with the CD calculation) and all of the extended conformers exhibit positive values in a range of +20° to +80°. The calculated signs are in accordance with the experimental values reported previously (+14.6°; *c* 0.10, dichloromethane, 25 °C),[15] while the magnitude is considerably overestimated. The deviation of the specific rotation (averaged over the conformers) calculated for the extended monomer (+63.2°) is slightly larger than the typical deviations reported for the commonly used test sets,[7] which may be attributable to the incorrect calculated population of the conformers or the solvent effect as well as neglect of vibrational contributions. As pointed out above in the calculation of CD spectra (vide supra), a substantial scaling (reduction) of the calculated $[\alpha]_D$ should be applied, if one considers the contributions of the folded conformers.

Geometrical Optimization of the CT-Dyad Dimer and Calculation of CD Spectra. It is known that the present CT-dyad tends to dimerize in dichloromethane at low temperatures, which is diagnosed by the appearance of a new band at ca. 480 nm with a strong negative Cotton effect.[15] By B3-LYP/6-31G-(d) optimization, we have already shown that two CT-dyad molecules form a dimer complex in a head-to-tail fashion.[15] In the present study, we optimized the dimer structures of the CT-dyad with the dispersion-corrected DFT-D method using the TZV2P basis set. Figure 4 illustrates the six optimized structures obtained by starting from the most stable extended conformers **E1**−**E3** (the other conformers of <5% contribution were ignored). Each dimer can form a pair of conformers by combining two molecules either from the less-hindered (thus favored) or the opposite face. The subsequent single-point SCS-MP2/TZVPP calculations were also performed with these optimized structures to obtain the relative energy difference (Table 3). The good agreement of the energies calculated by SCS-MP2 and DFT-D methods indicates that the DFT-D method provides quite reliable results even for such a large dimeric species with strong donor−acceptor interactions. Table 3 reveals that three out of six conformers (**D1**−**D3**) are close in energy (within ~2 kcal/mol), while the other three conformers (**D4**−

(35) (a) Dunning, T. H. *J. Chem. Phys.* **1993**, *98*, 7059−7071. (b) Kendall, R. A.; Dunning, T. H.; Harrison, R. J. *J. Chem. Phys.* **1992**, *96*, 6796−6806.

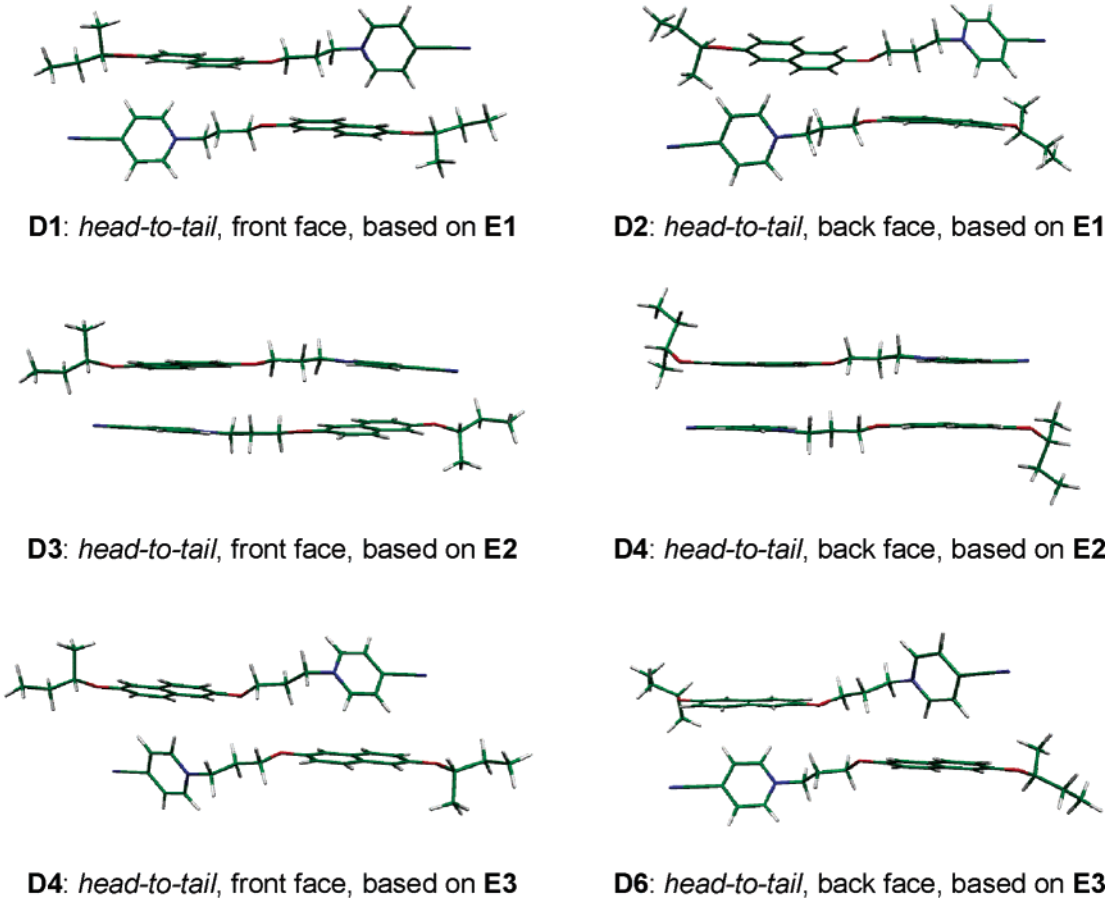

FIGURE 4. DFT-D-BLYP/TZV2P optimized structures of six conformations of the CT-dyad dimer.

TABLE 3. Relative SCS-MP2 and DFT-D Energies (in kcal/mol) and Relative Boltzmann Populations of the CT-Dyad Dimer in the Gas Phase and in Dichloromethane (COSMO Model)

	SCS-MP2	% population	SCS-MP2 (COSMO)[a]	% population	DFT-D	% population	DFT-D (COSMO)[a]	% population
D1	≡0	67.4	≡0	17.1	≡0	40.3	≡0	10.6
D2	1.05	23.6	0.99	6.4	0.54	23.4	0.19	8.7
D3	2.02	8.9	−1.49	76.3	0.11	36.1	−2.03	80.5
D4	12.62	0.0	8.57	0.0	8.49	0.0	5.97	0.0
D5	7.66	0.0	5.78	0.1	6.75	0.1	4.85	0.1
D6	7.56	0.0	5.95	0.1	6.74	0.1	5.11	0.1

[a] COSMO model with ϵ values of 8.93 (dichloromethane) was employed for the calculation.

D6) are much higher in energy by >7.5 kcal/mol. Therefore, only three stable conformers were subjected to further CD calculations. It is interesting to note that two sets of the donor−acceptor pairs are not face-to-face stacked but are oriented perpendicularly in the most stable conformers (**D1** or **D2**), while the less-stable conformers (**D3** and **D4**) are face-to-face stacked (although the latter form is more frequently found in crystals),[36] probably due to the steric repulsion between the linker methylene chains (see Figure S2 in the Supporting Information for top-view projections).

The CD spectra calculated at the BH-LYP/TZV2P level for dimers **D1**−**D3** are shown in Figure 5. Most interestingly, the calculated spectra of the isomeric **D1** and **D2** are nearly mirror-imaged (Figure 5, left). Because a critical balance of the isomer distribution determines the overall spectral shape of the CD, it is quite important to work with the reliable relative energies between the conformers. Most of the transitions found in the CD spectrum calculated for the face-to-face dimer **D3** are red-shifted relative to those of the perpendicular conformers (**D1** and **D2**), as a consequence of the better overlap between the donor and acceptor moieties in **D3** (see also Figure S2 in the Supporting Information).

A close examination of the important transitions found in the most stable dimer **D1** (see also Table S1 in the Supporting Information) shows that the bands A−D indicated as bars in Figure 5 (right) (see also Figure S3 (left) in the Supporting Information for isomer **D3**) correspond to the HOMO → LUMO, HOMO−1 → LUMO, HOMO → LUMO+1, and HOMO → LUMO+2 excitations, respectively. From the

(36) (a) Rathore, R.; Lindeman, S. V.; Kochi, J. K. *J. Am. Chem. Soc.* **1997**, *119*, 9393−9404. (b) Yoshikawa, H.; Nishikiori, S.; Ishida, T. *J. Phys. Chem. B* **2003**, *107*, 9261−9267.

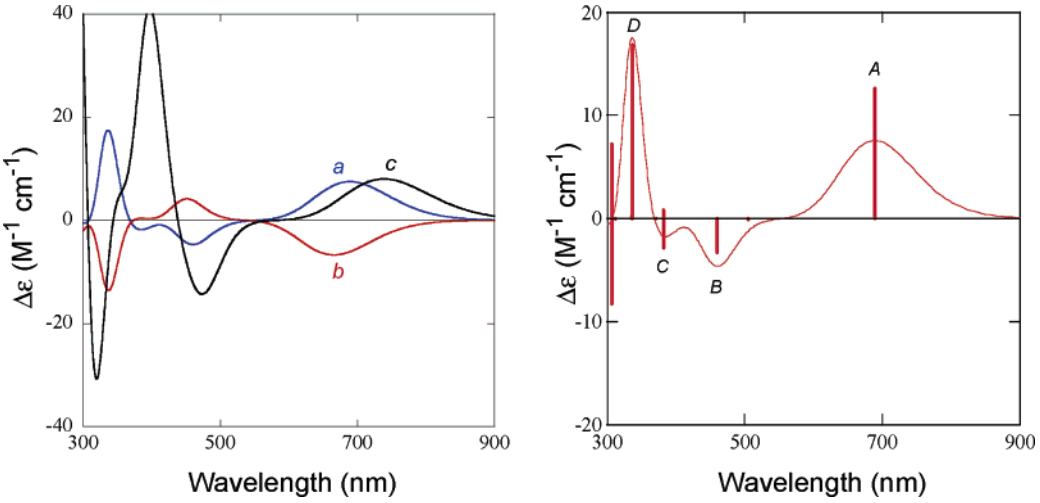

FIGURE 5. Left: Calculated CD spectra at BH-LYP/TZV2P level for the major conformers: (a) **D1**, (b) **D2**, and (c) **D3**. Right: The simulated CD spectra and bar-representation of the excitation energies and rotatory strength of the transitions for the most abundant conformer **D1**.

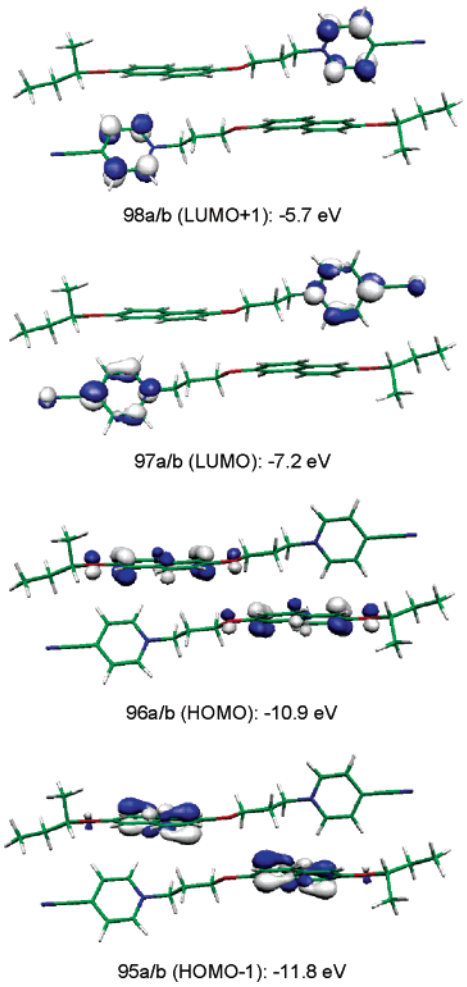

FIGURE 6. Molecular orbitals involved in the first 10 transitions of **D1**. Note that molecular orbitals of *b* symmetry are omitted for clarity; they are essentially the same as those of *a* symmetry (shown above) but different only in sign (color) of one of the molecules in the dimer.

relevant molecular orbitals shown in Figure 6, we can assign the bands A−C to the formal charge-transfer transitions (donor-to-acceptor excitation), while the band D to a local excitation ($\pi-\pi^*$) of the naphthalene moiety.

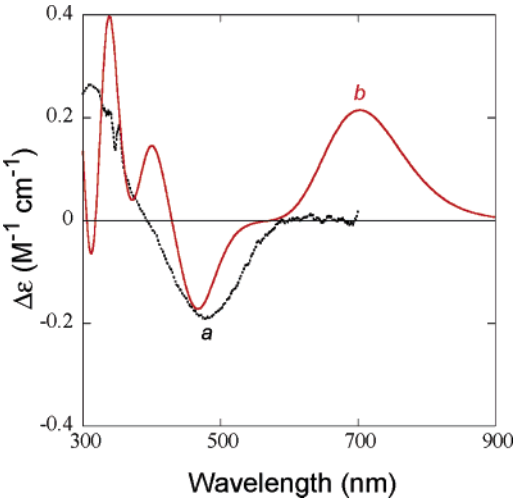

FIGURE 7. Comparison of (a) experimental and (b) calculated CD spectra at the BH-LYP/TZV2P level for the dimer of the CT-dyad. The calculated spectrum was obtained by averaging three major conformers (**D1**−**D3**) with a scaled intensity 1/20. Experimental spectrum of the dimer was obtained in dichloromethane at −95 °C.

An average spectrum of the dimer is compared with the experimental CD spectrum recorded in dichloromethane at −95 °C, shown in Figure 7. The almost perfect agreement between the theoretical and experimental spectra demonstrates the validity of the TD-DFT method for this purpose. The lack of band A in the experimental CD spectrum is clearly due to the instrumental limitation of the spectrometer used, and the detection and analysis of such a strong Cotton effect in the visible range are planned in related donor−acceptor systems. Use of the B3-LYP functional in the CD calculations of dimers **D1**−**D3** was unsuccessful, due to the substantial underestimation of the transition energy (see Figure S4 in the Supporting Information for the detailed B3-LYP results). This is consistent with the previous report on the charge-transfer excited-state calculations by the TD-DFT method.[23]

Examination of the Solvent Effect with the COSMO Model. Dielectric continuum solvation models (CSMs) such as PCM or COSMO (conductor-like screening model) have turned out to be elegant and efficient methods for the inclusion of solvent effects in quantum chemical calculations. At costs

TABLE 4. Relative Boltzmann Distributions of the CT-Dyad Monomer in the Gas Phase and in Acetonitrile (COSMO Model)

method	relative distribution between folded and extended conformers Σ(folded):Σ(extended)	energy difference between most stable extended and folded monomer, kcal/mol
COSMO-SCS-MP2[a]	2.8 (73.9:26.1)	0.35
SCS-MP2	15.3 (93.9:6.1)	2.48
COSMO-DFT-D[a]	1.5 (60.6:39.4)	0.05
DFT-D	3.8 (79.0:21.0)	1.01

[a] COSMO model with ϵ values of 36.64 (acetonitrile) was employed for the calculation.

comparable to gas-phase calculations, they are generally capable of giving a surprisingly good description of the properties and energetics of molecules in various solvents.[32] The effect of solvent was also tested for conformer populations of both the monomer and the dimer of CT-dyad with the COSMO model. Since the experimental spectra of the monomer and dimer were recorded in acetonitrile and in dichloromethane, respectively, we have chosen the same solvents for the COSMO treatments. Tables 3 and 4 gather the effect of the CSM model on the relative energies and distribution of the conformers (see also Table S2 in the Supporting Information for more detailed data for the monomer). As summarized in Table 4, the preference for the folded monomer is less pronounced in acetonitrile (5 times with SCS-MP2 and 2 times with DFT-D), although the folded conformer is still preferred. The face-to-face conformer **D3** is much favored with respect to **D1** or **D2** in dichloromethane (Table 3). However, the CSM-based estimations of the conformer population of the dimer lead to poorer agreement with the experimental CD spectrum (see Figure S3 (right) in the Supporting Information). We suppose that the use of a continuum solvation model is not suitable to incorporate the solvent effects for the simulation of the CD spectra for conformatioanlly flexible systems, since the dynamic behavior of the molecules is completely ignored. The combined quantum mechanics/molecular mechanics models would be the alternative approach to quantitatively predict the optical properties of complex systems.[37]

Nevertheless, the present results clearly indicate that although all the calculations (geometrical optimization, relative energy, and spectral calculation) are done in the gas phase, the overall performance to reproduce the experimental CD spectra (in solution) is excellent. This is probably because the errors arising from the other factors, such as transition energy, rotatory strength, relative population, and optimized geometries, are much more crucial than the effect of solvent.

4. Summary and Conclusions

In the present study on the theoretical calculations of CD spectra of a flexible donor−acceptor (CT)-dyad system, we have demonstrated the following:

(1) The dispersion-corrected DFT-D method, which has previously proven to be quite valuable in describing weakly interacting molecular complexes, is also accurate and efficient in geometrical optimization of the donor−acceptor system. Thus, 12 monomer and 6 dimer conformations have been successfully optimized within a quite reasonable computation time.

(2) The density functionals with relatively high fractions of exact exchange (BH-LYP) and the use of Boltzmann distributions based on the SCS-MP2 energies are necessary for accurately reproducing the CD (and UV−vis) spectra of both CT-dyad monomer and dimer. The CD calculations predict a new transition in the near-IR region for the dimer complex, which is a future target for experimental detection.

(3) The CD calculations with the popular B3-LYP functional confirm the small population of the folded conformer(s) of monomeric CT-dyad in solution, while the use of this functional leads to serious underestimations of CT transition energies. The B3-LYP simulated CD spectra of the dimer do not show any similarity with the experimental data.

(4) The CSM-based model slightly changes the relative distribution between the folded and extended conformers for the monomer, but results in a poorer agreement of the CD spectrum for the dimer. The errors arising from the other factors, such as transition energy, rotatory strength, relative population, and optimized geometries, are much more crucial than the effect of solvent. Nevertheless, the calculations in the gas phase by the present-day TD-DFT method are capable of reproducing the experimental CD spectra of the present donor−acceptor dyad (in solution) almost perfectly.

In conclusion, the combination of the DFT geometry optimization, single-point SCS-MP2 energy, and TD-DFT CD calculations is a versatile and powerful tool for the conformational analysis of chiral molecules. For large molecules or aggregates, the following general strategy is recommended: (i) dispersion-corrected DFT-D geometrical optimization of the weakly bonded complex, (ii) single-point SCS-MP2 energy calculation to obtain the conformer population, (iii) calculation of CD spectra with the BH-LYP functional, and (iv) use of basis sets of triple-ζ quality with appropriate polarization functions in all three steps. Accordingly, the combined use of the experimental CD spectra and the theoretical simulation by the state-of-the-art TD-DFT calculations described here provides us with an extremely useful and reliable method for determining the absolute configuration and analyzing the molecular and supramolecular conformation of medium-to-large molecules and molecular assemblies in solution. Further applications of this strategy to the conformational analysis of relatively large and flexible molecules are currently in progress.

Acknowledgment. T.M. thanks the Alexander von Humboldt-Stiftung for the fellowship. We thank Drs. Christian Mück-Lichtenfeld, Christian Diedrich, and Manuel Piacenza for technical assistance and fruitful discussion. Financial support of this work by a Grant-in-Aid for Scientific Research from the Ministry of Education, Culture, Sports, Science, and Technology of Japan (No.16750034, to T.M.) is gratefully acknowledged.

Supporting Information Available: Details of the calculated CD spectra of the CT-dyad, projection of some conformers and excited-state properties of the dimer, details on the solvent effect on the monomer CT-dyad, and Cartesian coordinates of all optimized geometries of the CT-dyad. This material is available free of charge via the Internet at http://pubs.acs.org.

JO061855I

(37) (a) Sebek, J.; Kejik, Z.; Bour, P. *J. Phys. Chem. A* **2006**, *110*, 4702−4711. (b) Glattli, A.; Daura, X.; Seebach, D.; van Gunsteren, W. F. *J. Am. Chem. Soc.* **2002**, *124*, 12972−12978. See also: Pecul, M.; Marchesan, D.; Ruud, K.; Coriani, S. *J. Chem. Phys.* **2005**, *122*, 024106.